Macrocyclic Molecular Rotors with Bridged Steroidal Frameworks

ARTICLE *in* THE JOURNAL OF ORGANIC CHEMISTRY · OCTOBER 2012

Impact Factor: 4.72 · DOI: 10.1021/jo3020402 · Source: PubMed

6 AUTHORS, INCLUDING:

Dorota Czajkowska-Szczykowska
University of Bialystok
9 PUBLICATIONS **52** CITATIONS
SEE PROFILE

Braulio Rodríguez-Molina
Universidad Nacional Autónoma de México
15 PUBLICATIONS **160** CITATIONS
SEE PROFILE

Miguel A Garcia-Garibay
University of California, Los Angeles
226 PUBLICATIONS **4,830** CITATIONS
SEE PROFILE

JOC The Journal of Organic Chemistry

Featured Article

pubs.acs.org/joc

Macrocyclic Molecular Rotors with Bridged Steroidal Frameworks

Dorota Czajkowska-Szczykowska,[†] Braulio Rodríguez-Molina,[‡] Nancy E. Magaña-Vergara,[§] Rosa Santillan,[§] Jacek W. Morzycki,*[,†] and Miguel A. Garcia-Garibay*[,‡]

[†]Institute of Chemistry, University of Białystok, Piłsudskiego 11/4, 15-443 Białystok, Poland

[‡]Department of Chemistry and Biochemistry, University of California, Los Angeles, California 90095, United States

[§]Departamento de Química, Centro de Investigación y de Estudios Avanzados del IPN, México D.F. Apdo. Postal 14-740, 07000 Mexico

Supporting Information

ABSTRACT: In this work, we describe the synthesis and solid-state dynamics of isomeric molecular rotors **7*E*** and **7*Z***, consisting of two androstane steroidal frameworks linked by the D rings by triple bonds at their C17 positions to a 1,4-phenylene rotator. They are also linked by the A rings by an alkenyl diester bridge to restrict the conformational flexibility of the molecules and reduce the number of potential crystalline arrays. The analysis of the resulting molecular structures and packing motifs offered insights of the internal dynamics that were later elucidated by means of line shape analyses of the spectral features obtained through variable-temperature solid-state ^{13}C NMR; such analysis revealed rotations in the solid state occurring at kilohertz frequency at room temperature.

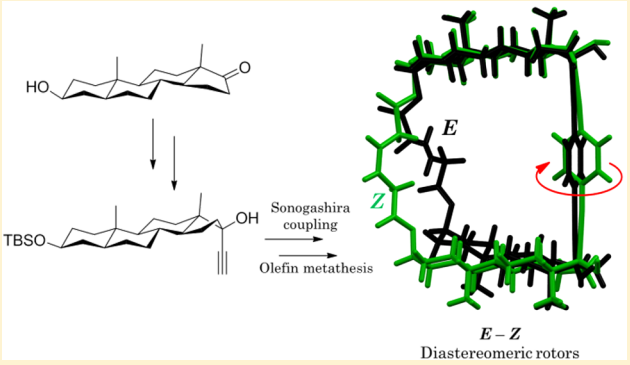

INTRODUCTION

The successful design of dynamic processes at the molecular level will be fundamental for the development of molecular machines and functional materials.[1] It has been suggested that the control of molecular rotation and reorientation in condensed-phase matter can lead to the modulation of dielectric and photonic responses in crystalline materials.[2,3] Over the past few years, we have made progress on the design, synthesis, and dynamic characterization of molecular rotors that bear a structural resemblance to macroscopic gyroscopes[4,5] and compasses.[6] Based on a molecular design that integrates a *rotating unit* that is covalently bound by a dialkynyl *axle* to relatively large and static groups that shield the rotator and act together as a *stator,* we have obtained crystalline solids with rotational frequencies that vary from a few hertz to several gigahertz.[7,8] To convey the coexistence of highly dynamic components and static, lattice-forming frameworks, we have suggested the term *amphidynamic crystals*.[7,9]

In our search for new *amphidynamic* architectures, we have recently begun exploring the use of steroidal stators.[10] Among several possible advantages, one may include their structural rigidity, their homochirality, and the availability of alkynyl-substituted structures (originally developed as contraceptives). The steroidal rotors previously described[10,11] consist of two 17α-ethynyl-substituted steroidal stators linked by a central 1,4-phenylene that acts as a rotator (Figure 1a). It is expected that the homochiral structures of these compounds will guarantee the formation of *noncentrosymmetric* crystalline arrays, which are a prerequisite for piezoelectricity, ferroelectricity, and second-order nonlinear optical responses, among other properties that are only present in polar crystal structures.[3,12] Regarding rotational dynamics, it has been demonstrated that the phenylene rotators partially shielded by steroidal derivatives range from static,[10] to one example where they rotate in the solid state at room temperature at megahertz frequencies and in a correlated manner.[11] The use of steroids can also be advantageous since their chemical transformations have been extensively explored due to their broad application in the synthesis of hormones,[13] vitamin D derivatives,[14] transporters,[15] etc. Many steroids play a significant role in phytotherapy as antiviral,[16] antibacterial,[17] antifungal,[18] or antitumoral compounds.[19] Lately, they have been used as promising building blocks for the synthesis of biomaterials and macrocycles with ion-recognition properties.[20]

One of the concerns about the use of 17α-ethynyl-substituted steroidal stators such as the one represented in Figure 1a comes from the conformational flexibility that exists as a result of the relatively free rotation of the two steroidal units about their linking triple bonds. The availability of many different orientations, with only *syn-* and *anti-* shown in Figure 1, may result in the formation of different conformational polymorphs,[21] as well as in close intermolecular contacts involving the rotator. Considering this, we describe here the synthesis and characterization of two structures where this conformational degree of freedom is prevented by a macro-

Received: September 17, 2012
Published: October 21, 2012

   dx.doi.org/10.1021/jo3020402 | J. Org. Chem. 2012, 77, 9970–9978

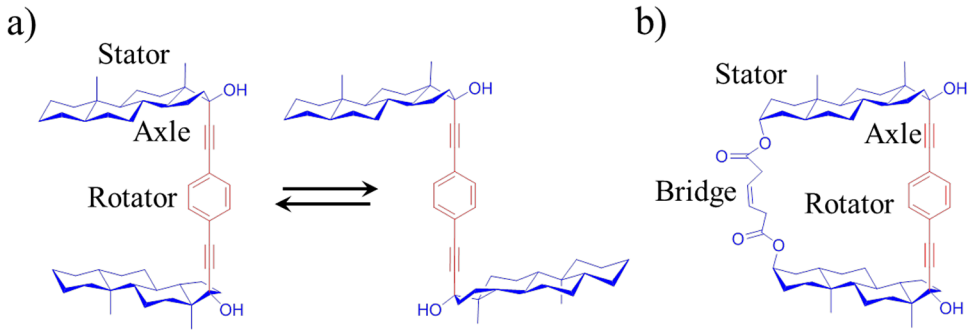

Figure 1. Line diagram of (a) conformationally unrestricted steroidal molecular rotors and (b) structure of one of the conformationally restricted molecular rotors studied in this work.

Scheme 1. Synthesis of compounds 2-4

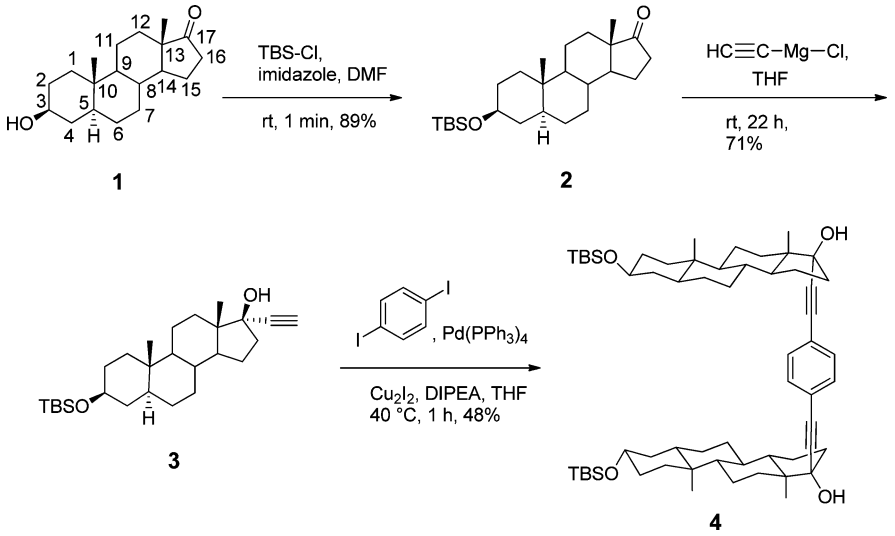

cyclic bridge, as shown in Figure 1b. The desired structures **7*E*** and **7*Z*** consist of two molecules of 17α-ethynyl-5α-androstan-17β-ol (stator) that are linked at the alpha faces of the D rings by a 1,4-phenylene (rotator) and also at the α faces of the A rings by side chains with ester and double bond functionalities. We report an efficient seven-step synthesis of the isomeric molecular rotors with the bridge obtained in the final step by olefin metathesis, giving rise to *cis* and *trans* (**7*E*** and **7*Z***, respectively) alkenes.[20a,22] The structural differences arising from the double-bond configuration in molecular rotors **7*E*** and **7*Z*** correlate with the position of the steroidal fragments in the solid state, as revealed by single-crystal X-ray diffraction. Using differential scanning calorimetry (DSC) and thermogravimetric analysis (TGA) methods, we determined the thermal stability of their corresponding solid forms, and taking advantage of variable-temperature solid-state ^{13}C NMR CPMAS, we were able to explore their rotational dynamics, which revealed a phenylene 180° rotation in the kilohertz regime at ambient temperature in the case of molecular rotor **7*Z*** with an activation energy of 7.19 kcal/mol.

RESULTS AND DISCUSSION

Synthesis and Characterization. As a starting point in the synthesis of molecular rotors **7*E*** and **7*Z***, we selected the commercially available and relatively inexpensive 3β-hydroxy-5α-androstan-17-one (**1**). The hydroxyl group in **1** was protected as the *tert*-butyldimethylsilyl ether to obtain **2** (Scheme 1).[23] Compound **2** was then reacted with ethynylmagnesium chloride in dry THF at room temperature with the addition of the acetylide onto the α face, directed by the methyl group at C13 to give compound **3** in 71% yield. It is well-established that alkynylation of 17-oxo steroids generally proceeds by attack of the organometallic reagent from the less hindered α side of the keto group, giving almost exclusively the 17α-alkenyl-17β-ol derivatives.[24] Infrared spectroscopy of **3** revealed characteristic stretching bands for the hydroxyl group at 3597 cm^{-1} and for the free alkyne at 3305 cm^{-1}. The solution ^{1}H NMR spectra exhibited characteristic signals at δ = 3.60−3.50 (broad m, 1H) attributed to the axial proton H-3α and the signal at δ = 2.57 (s, 1H) from the proton in the free alkyne fragment. Additionally, the presence of the silyl-protecting group was evidenced by the signals at δ = 0.89 (s, 9H) and δ = 0.05 (s, 6H), from the *tert*-butyl and methyl substituents, respectively. ^{13}C NMR spectra confirmed the presence of the alkyne group with signals observed at 87.7 and 73.8 ppm with chemical shifts analogous to those found in similar structures. High resolution mass spectrometry showed a peak at m/z = 453.3176 that corresponds to the expected molecular ion. Subsequent reaction of **3** with 1,4-diiodobenzene following Sonogashira conditions using Pd(0) under inert atmosphere yielded **4** in 48% (Scheme 1). In addition to the signals observed in the precursor **3**, the ^{1}H NMR spectrum of **4** confirmed the coupling of the phenylene ring to the steroidal framework, as revealed by the aromatic signal at δ = 7.38 (s,

dx.doi.org/10.1021/jo3020402 | J. Org. Chem. 2012, 77, 9970−9978

Scheme 2. Synthesis of Compounds 5 and 6 and Macrocyclic Molecular Rotors 7*E* and 7*Z*

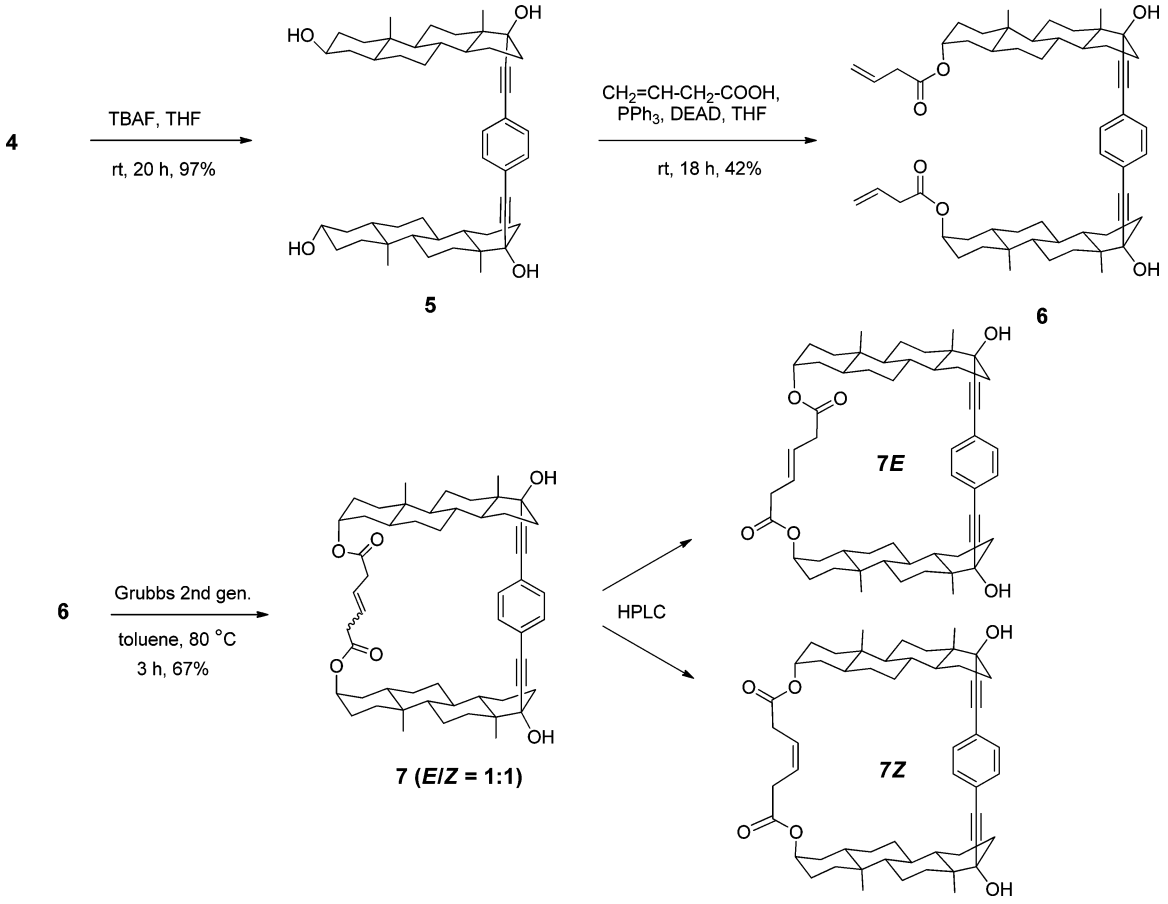

4H). The ^{13}C NMR spectrum also showed two distinctive signals at δ = 131.5 and δ = 122.8 that correspond to the protonated and *ipso* aromatic carbon atoms, respectively. HRMS gave a m/z peak at 957.6611 that matches the proposed formula with two steroids surrounding the 1,4-diethynylphenylene portion.

The silyl-protecting groups in compound **4** were easily removed using tetrabutylammonium fluoride (TBAF) to give **5** with the free β-hydroxyl at C3 in high yield (97%), as depicted in Scheme 2. The loss of two *tert*-butyldimethylsilyl groups was confirmed by HRMS showing a peak at m/z = 729.4828 that corresponds to the expected mass for **5**. Subsequently, the Mitsunobu esterification[25] of the hydroxyl groups at C3 with successful inversion of configuration using 3-butenoic acid, diethyl azodicarboxylate (DEAD), and triphenylphosphine afforded diester **6** in 42% yield. The Mitsunobu reaction is widely used in natural product synthesis since it proceeds with clean inversion of stereogenic centers in the secondary alcohols including saturated steroidal 3β-alcohols.[26] It must be noted that the length of the side chains was chosen by inspection of Dreiding models, and reinforced by molecular modeling using the MM+ force-field (HyperChem),[27] in order to subsequently obtain the smallest macrocycle with the lowest strain. Infrared spectroscopy showed the stretching bands from the hydroxyl groups at 3597 cm^{-1} and from the ester groups shifted at 1722 cm^{-1}. Besides the signals from the steroid backbone and aromatic ring, ^{1}H NMR exhibited signals at δ = 6.00−5.90 (m, 2H), 5.20−5.16 (m, 2H), and 5.15−5.13 (m, 2H) corresponding to six vinyl protons. The narrow signal of two equatorial protons H3β at δ = 5.05 ($W_{1/2}$ = 7 Hz), compared with a broad signals of axial 3α-protons in **4** ($W_{1/2}$ = 24 Hz), confirmed the inversion of configuration at this stereogenic center. The ester function could also be identified by solution ^{13}C NMR with signals at δ = 171.0 for the carbonyl, and 130.6 and 118.2 ppm from the vinyl carbons. HRMS analysis showed an m/z peak at 865.5347 that corresponds to the expected molecular ion of compound **6** clustered with sodium ion.

After attaching the esters chains with the proper length and in proper orientation, we carried out an olefin metathesis to afford diastereoisomeric compounds **7*E*** and **7*Z*** in a ratio ca. 1:1 due to the nonstereoselective route of the reaction using a Grubbs second-generation catalyst (Scheme 2). Different catalysts (Grubbs first generation, Hoveyda−Grubbs second generation) gave lower yields and comparable stereoselectivity. After purification by HPLC, the diastereomeric molecular rotors **7*E*** and **7*Z*** could be distinguished by small spectroscopic differences. The infrared spectra taken in $CHCl_3$ showed stretching bands for the ester groups at 1721 and 1725 cm^{-1} for the isomers ***E*** and ***Z***, respectively. Also, the ^{1}H NMR signal of the olefinic protons of compound **7*E*** appeared at δ = 5.73 (2H, m) and that of compound **7*Z*** was observed at δ = 5.87 (2H, m). Another difference could be noticed in the ^{13}C NMR spectrum, where the signal of the vinyl carbon atoms of rotor **7*E*** appeared at δ = 126.0 while the analogous signal of molecular rotor **7*Z*** was found at δ = 124.0. As expected, the high resolution mass spectra of both isomers confirmed the formula showing molecular ions as clusters with a sodium ion (m/z = 837.5058).

After crystallization experiments, analysis of the molecular rotors **7*E*** and **7*Z*** in the solid state was carried out in order to

dx.doi.org/10.1021/jo3020402 | *J. Org. Chem.* 2012, 77, 9970−9978

establish a connection between structure and dynamics for each diastereoisomer. As detailed below, the analyses consisted of single crystal and powder X-ray diffraction experiments, differential scanning calorimetry and thermogravimetric analyses, infrared and variable-temperature ^{13}C CPMAS experiments.

Solid-State Characterization of Molecular Rotors 7*E* and 7*Z*. *Single-Crystal X-ray Diffraction Studies.* Single crystals of molecular rotors 7*E* and 7*Z* suitable for X-ray diffraction studies were grown by slow evaporation of a saturated solution in dichloromethane. The ORTEP diagrams derived from data acquired at 293(2) K are illustrated in Figure 2. Compound 7*E* was solved in the monoclinic space group $P2_1$

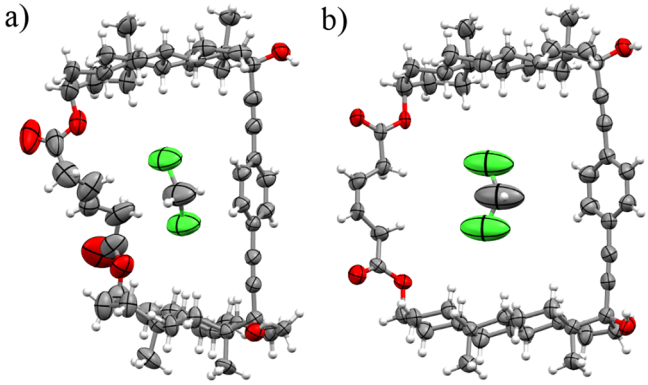

Figure 2. ORTEP diagrams of macrocyclic molecular rotors: (a) compound 7*E* with the dichloromethane molecule in one of the disordered positions and (b) compound 7*Z* with the dichloromethane molecule. The ellipsoids are drawn at 50% probability.

with one molecule per asymmetric unit and two molecules in the unit cell. The anisotropic refinement also showed one dichloromethane molecule disordered over three positions. On the other hand, isomer 7*Z* was refined in the orthorhombic space group $P2_12_12_1$ with one molecule per asymmetric unit and four molecules in the unit cell. This compound also contained one dichloromethane molecule located inside the macrocyclic cavity but without noticeable disorder.

A comparison between the molecular structures of macrocyclic rotors revealed that the 1,4-diethynylphenylene fragments are close to linear (7*E* = 178.3° and 7*Z* = 173.2°) and relatively distant from the bridging chain, suggesting that different rotational dynamic would have to arise from differences in packing effects, rather than from intramolecular interactions with the bridge. In both molecular rotors, the chain was disordered over two positions with a 50:50 occupancy, as is commonly observed in flexible fragments containing alkene functionalities.[28]

Regardless of the position of the disordered side chain, *trans* substitution in the *E* isomer causes the bridge to acquire a conformation similar to a distorted "S", which places the two steroids in a staggered position relative to the diethynyl molecular axis. In contrast, the side chain in the *Z* isomer adopts a "U" arrangement allowing for a nearly eclipsed location of the steroids. Each isomer presented different distances between the edges of the steroid fragments with compound 7*E* having a C3−C3′ distance of 9.41 Å, which is shorter than the 10.09 Å distance observed in 7*Z* (see the Supporting Information).

The macrocyclic molecular rotors 7*E* and 7*Z* present very distinctive packing arrays in their corresponding crystals. Their packing arrangement can be described as a combination of normal OH···O and "weak" CH···O hydrogen bonds[29] that hold the molecules together. Rotor 7*E* (space group $P2_1$) packs in columns with opposite tilt having the screw axis along the *a*,*c* plane, placing the 1,4-diethynylphenylene molecular axis roughly parallel to the *a*,*b* plane (Figure 3a). These columns act as a channel that is occupied by the dichloromethane molecules in the lattice. The rotators of 7*E* face each other and one CH of the central phenylene interacts with a neighboring hydroxyl group with donor−acceptor distance (D−A) of 3.289 Å and a DHA angle (∠) of 154.6°. Molecular rotors in adjacent columns interact in a zigzag manner through OH···O interactions between their hydroxyl groups at C17, with donor−acceptor distances of 3.020 Å and DHA angles of 135.3°. It is possible that the short distances between columns and rotators can somewhat restrict the motion of the rotators in this arrangement.

The molecular rotor 7*Z* packs in perpendicular interpenetrating layers with the rotator fragment facing toward the next coplanar neighboring bridge (Figure 3b). From the X-ray data, it can be postulated that the array in 7*Z* may enable faster rotational dynamics in the solid state as compared to its isomer 7*E*, possibly due to the flexible side chain that could bend if necessary. In a following section, it will be shown that the double-bond proximity to the neighboring rotator plays a major role defining the internal rotation. In this arrangement, the 1,4-diethynylphenylene molecular axis also lies roughly parallel to

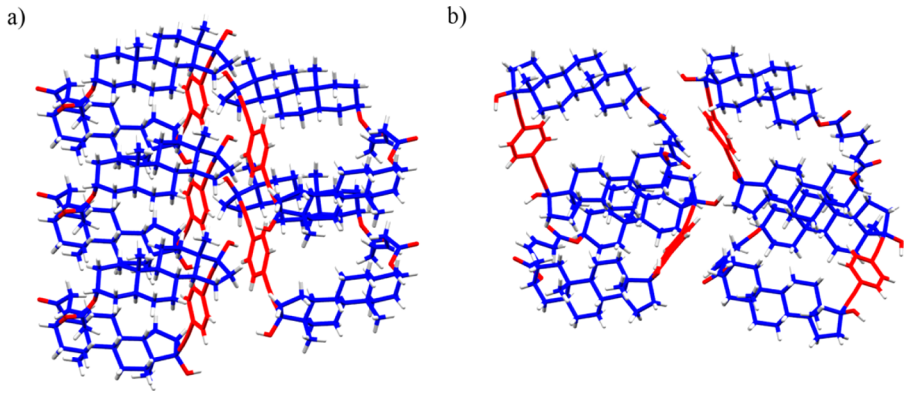

Figure 3. Crystal packing of molecular rotors: (a) 7*E* showing a columnar packing and (b) 7*Z* with an interpenetrated array. The dichloromethane molecules contained in both structures were removed for clarity.

dx.doi.org/10.1021/jo3020402 | J. Org. Chem. 2012, 77, 9970−9978

the *a*,*b* plane as in the isomer ***E***. Similarly, the hydroxyl groups at C17 of neighboring rotors interact with each other with D−A distance of 2.873 and ∠ D−A of 172.9°. Additional distances and angles of the observed intermolecular interactions in compounds **7*E*** and **7*Z*** can be found in the Supporting Information.

Powder X-ray Diffraction Experiments and Solid-State IR. Solid samples of **7*E*** and **7*Z*** resulting from crystallization experiments were studied by X-ray powder diffraction and infrared spectroscopy (ATR) before and after variable-temperature solid-state NMR, to ensure the identity and integrity of the crystal forms. Bulk solids obtained after slow evaporation from dichloromethane presented powder patterns with sharp Bragg reflections and narrow peaks in the range 5−55° (2θ degrees) that matched very well those calculated from the X-ray single-crystal diffraction structures (see the Supporting Information). Moreover, even though molecular rotors **7*E*** and **7*Z*** showed minimal differences in their IR spectra when taken in $CHCl_3$ solution, the two solid forms gave specific stretching bands in the solid-state infrared spectra, especially those corresponding to the hydroxyl groups at 3538 and 3426 cm^{-1} for **7*E*** and **7*Z***, respectively. Interestingly, while the carbonyl group in crystalline **7*E*** showed one band at 1737 cm^{-1}, two bands at 1737 and 1712 cm^{-1} were observed for the solid compound **7*Z*** (see the Supporting Information).

Thermal and Calorimetric Analyses. The thermal stability of crystalline samples of molecular rotors **7*E*** and **7*Z*** was explored using differential scanning calorimetry (DSC) and thermogravimetric analyses (TGA) to accurately corroborate the visual melting point and to detect phase or glass transitions upon temperature changes. More importantly, this stability assessment was used to determine the temperature range that the sample can be submitted to in variable-temperature solid-state NMR experiments.

Calorimetric experiments for both compounds indicated some transitions, but the changes were very small and gradual. Conversely, thermogravimetric analysis confirmed that the steroidal molecular rotor ***E*** is stable upon heating from room temperature up to 175 °C. When this temperature is reached, the sample starts to lose mass until 295 °C, with a 5.3% weight loss in this interval attributed to the evolution of dichloromethane molecules. This suggests that partial and gradual desolvation of the bulk solid can occur during storage, reducing the amount of CH_2Cl_2 within the lattice from the 9% value suggested by the X-ray experiment. Above 300 °C, the sample presents concomitant melting and decomposition, as suggested by the abrupt loss of weight, a result that agrees with the visual melting point measurement when the sample shrinks and darkens progressively after 300 °C. Similarly, loss of solvent in compound **7*Z*** started at about 175 °C and ended at ca. 232 °C, with a total mass loss of 7.0%. After losing solvent, the solid sample remains stable up to ca. 300 °C, when melting and decomposition occur (see the Supporting Information).

Variable-Temperature Solid-State ^{13}C NMR CPMAS. After having confirmed the thermal stability of macrocyclic rotors, we submitted samples with the appropriate solid form ($P2_1$ or $P2_12_12_1$ for rotors ***E*** and ***Z***, respectively) to solid-state NMR experiments to explore the rotational dynamics of the 1,4-phenylene. It is well-known that line shape analysis of variable-temperature ^{13}C NMR spectra is a suitable technique to document the dynamics of site exchange processes occurring in the ca. 100−1000 Hz regime.[1d,30] Conveniently, only the rotator signals of **7*E*** and **7*Z*** appear in the aromatic region of the spectra between 127 and 137 ppm.

Most carbon signals in the solid-state spectra occur in sets of two, indicating that analogous carbons from the two steroids in the molecule are magnetically nonequivalent, in agreement with crystallographic information showing that both macrocyclic rotors **7*E*** and **7*Z*** contain one molecular rotor per asymmetric unit. The room-temperature ^{13}C CPMAS spectrum of compounds **7*E*** (Figure 4, top) and **7*Z*** (bottom) showed that

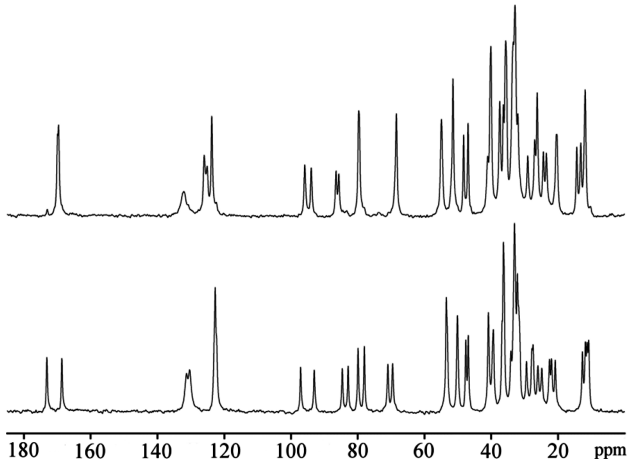

Figure 4. ^{13}C NMR CPMAS spectra at room temperature of macrocyclic rotors **7*E*** (top) and **7*Z*** (bottom) from recrystallization in dichloromethane.

not all of their signals were resolved, despite being relatively narrow (FWHM = 30−35 Hz). The symmetry of the two structures also requires the four CH rotators carbons to be magnetically nonequivalent under static conditions, although it had to be recognized that limited chemical shift dispersion would result in strong spectral overlap. Additional experiments using the nonquaternary suppression technique[31] to reveal only signals corresponding to nonprotonated and highly mobile carbons (see the Supporting Information), allowed us to identify several signals from the spectra and confirm their assignment by comparison with those previously assigned in solution NMR experiments. From these analyses, it was corroborated that the rotator signal coming to the CH carbons of isomeric rotors **7*E*** and **7*Z*** appear at ca. 137−127 ppm and are sufficiently separated from other signals to make it potentially possible to characterize the phenylene rotational dynamics using variable-temperature measurements.

As a starting point to address the effects of rotational exchange on the line shape of the aromatic CH signals, we noticed that the ^{13}C CPMAS NMR spectrum for macrocyclic rotor **7*E*** at 298 K has only one broad signal, suggesting that there is not enough chemical shift dispersion to clearly distinguish different sites or that there is a rotational process in the intermediate exchange regime. Although lowering the temperature to 173 K failed to split the signal, going above 298 K progressively sharpened it until two peaks could be partially resolved with a separation of 29 Hz (0.39 ppm) at 323 K. This suggests a process where intermediate rotator dynamics begins to enter the fast exchange regime (see the Supporting Information). Higher temperatures narrowed the signals slightly until they began to lose intensity by 403 K, presumably due to spin−lattice relaxation in the rotating frame ($T_{1\rho}$). Efficient spin−lattice relaxation in the rotating frame as a result

dx.doi.org/10.1021/jo3020402 | J. Org. Chem. 2012, 77, 9970−9978

of motions in the 10−20 kHz regime has the effect of destroying the magnetization while the corresponding ^{13}C signals are being accumulated by cross-polarization. In any event, we interpret the modest temperature dependence in the spectra of macrocyclic molecular rotor **7*E*** over a 230 K range (i.e., 173−403 K) as an indication of slow motion and large rotational barrier.

In contrast, the room-temperature ^{13}C CPMAS spectrum of compound **7*Z*** displayed two close aromatic signals at δ = 131.2 and δ = 130.3, suggesting that the rotator could be involved in a motional process with a frequency that averages the different magnetic environments at the two sides of the phenylene group in the NMR time scale (Figure 4, bottom). This speculation was confirmed with low-temperature ^{13}C CPMAS NMR experiments between 296 and 173 K, which showed the splitting of the two original signals into four as the temperature was lowered to 223 K. Additional experiments taken above room temperature revealed that the two signals first sharpen and then vanish progressively, as it was observed at high temperatures for compound **7*E***.

In order to correlate the observed line shape variations in the phenylene signals of compound **7*E*** with a dynamic exchange process, we selected experiments between 273 and 183 K to simulate their lineshapes with the WinDNMR software.[32] Our model is based on a 2 × 2 spin model, i.e., two pairs of singlets coalescing into two singlets with the same site exchange rate constant *k*. In this model, it was necessary to assign the signals involved in the exchange, prior to exploring their exchange rate. As represented in a cartoon manner in Figure 5, the signals AB

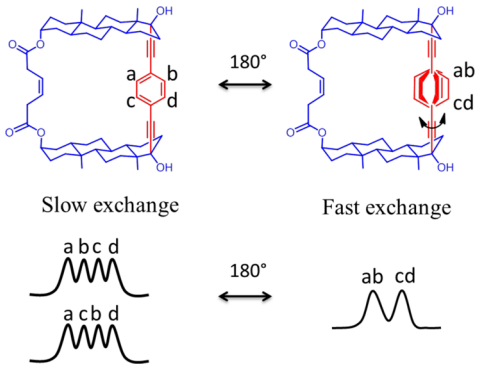

Figure 5. Diagram illustrating the two considered arrays of the four crystallographically and magnetically nonequivalent signals in the slow exchange regime that would coalesce into two signals in the fast exchange regime through a rotational process.

and CD in the fast exchange regime would arise from rotator carbon atoms A ↔ B and C ↔ D, that are related by 180° jumps. The order of those signals in the slow exchange regime from low field to high field could be ABCD or ACBD, as indicated in the bottom left portion of Figure 5, and we explored both possibilities. After several attempts, the best spectral simulations resulted when the exchange occurs between signals in the ABCD array as shown in Figure 6a.[33] However, it should be pointed out that the best simulations deviated from a simple model involving 180° jump between two sites that remain constant as a function of temperature. In fact, the difference in chemical shifts of the signals assigned to the static model had to be adjusted by as much as 6 Hz. This observation was attributed to small changes in the crystal structure due to conformational adjustments of the bridging

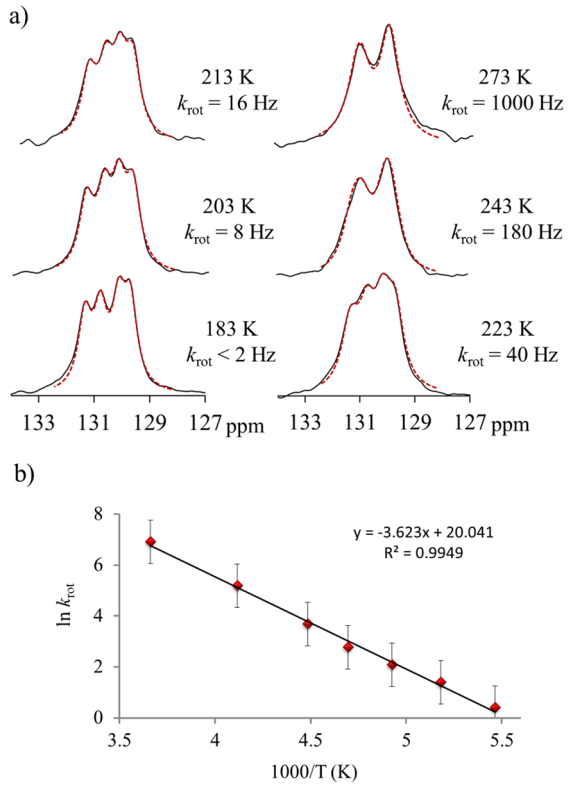

Figure 6. (a) Comparison between simulated and experimental line shapes of compound **7*Z*** from CPMAS ^{13}C NMR experiments between 273 and 183 K. (b) Arrhenius plot for the phenylene rotation in **7*Z*** with constants obtained from the simulation process. The corresponding activation energy and pre-exponential factor are 30.12 kJ/mol (7.19 kcal/mol) and 5.0 × 10^8 s^{-1}, respectively (R^2 = 0.99).

alkene diester. The single-crystal X-ray analysis of **7*Z*** suggested such motion of the side chain, which was confirmed by the ^{13}C NMR CPMAS experiments showing that the signal corresponding to the alkene carbons also change as a function of temperature variations. Unfortunately, the overlap of alkene signals with a quaternary carbon of the central phenylene at δ = 122.6 at room temperature prevented a complementary study of the double bond dynamics (see the Supporting Information).

Within the limits of the model, a comparison between the simulated and experimental rotator line shapes allowed us to obtain the exchange rate (k_{rot}) of the proposed 180° rotational motion, wich was subsequently used in an Arrhenius plot to calculate an activation energy (E_a) and a pre-exponential factor (A) of 7.19 kcal mol^{-1} and 5.0 × 10^8 s^{-1}, respectively. An Eyring plot (see the Supporting Information) gave an activation enthalpy $\Delta H^{\ddagger}$ of 28.26 kJ mol^{-1} (6.75 kcal mol^{-1}) and activation entropy $\Delta S^{\ddagger}$ of −84.20 J mol^{-1} K^{-1}. The low value for the pre-exponential factor and the value of $\Delta S^{\ddagger}$ suggest that rotation in **7*Z*** is not an elementary process in a constant potential but that it may require motion of the double bond in the bridge that affects directly the phenylene dynamics, as described above. A phenylene rotational barrier of 7.19 kcal/mol (30.12 kJ/mol) in crystalline **7*Z*** is much lower than that deduced in earlier examples involving norethisterone and ethisterone stators[10] but is higher than that of the molecular rotor based on mestranol.[11] The differences in activation energies can be explained in terms of the crystallographic arrangements: the ethisterone-based molecular rotors crystallize

dx.doi.org/10.1021/jo3020402 | J. Org. Chem. 2012, 77, 9970−9978

in one-dimensional layers due to the relative position (*anti*) of the steroidal fragments, with very limited space around the rotator.[10] On the other hand, the *syn* position acquired by the mestranol portions in the corresponding molecular rotor, gave rise to a helical array that allows the rapid reorientation of the phenylene.[11] The rotation of macrocyclic rotors **7*E*** and **7*Z*** presented here is located between those two ends of the dynamic behavior, favored by the steroidal conformation locked by the bridge that also helps to protect partially the rotator; however, the remaining intermolecular contacts are still important enough so as to increase the activation energy of the rotational process.

■ CONCLUSIONS

Molecular rotors **7*E*** and **7*Z*** with steroidal stators bridged by side chains with ene−dioate functionalities were designed and realized following a seven step synthesis. The *cis*/*trans* substitution of the bridge restricts the conformational degrees of freedom of the stators as conceived but this also exposes the rotator to intermolecular interactions in the solid state that affect their internal dynamics. The analyses of their different crystal structures suggested that tight interactions between adjacent rotators in **7*E*** can restrict their motion, while relatively looser phenylene-bridge interaction in the case of compound **7*Z*** may enable faster rotation. This hypothesis was corroborated by line shape analysis of their corresponding ^{13}C NMR spectral features in the solid state, which revealed that slow motion in **7*E*** occurs in the intermediate exchange at room temperature, while the phenylene rotator in **7*Z*** undergoes motion in the fast exchange regime at 273 K with a rotational activation barrier of 7.19 kcal/mol. With this information, the next generation of macrocyclic molecular rotors will be fine-tuned by implementing chemical transformations that protect the rotator from undesired interactions in the solid state.

■ EXPERIMENTAL SECTION

General Remarks. Melting points were determined on a Kofler apparatus of the Boetius type. NMR spectra were recorded in $CDCl_3$ solutions in 200 and 400 MHz spectrometers using the residual solvent as internal standard (only selected signals in the ^1H NMR spectra are reported). Infrared spectra were recorded on a FT-IR spectrometer in anhydrous chloroform solutions, as KBr pellets or as solid samples using the ATR technique. Mass spectra were obtained using an electrospray ionization technique using a time-of-flight detector or electron-impact (70 eV) analyzer. The reaction products were isolated by column chromatography performed on 70−230 mesh silica gel. Yields refer to chromatographically purified products unless otherwise stated. The HPLC separations of the isomeric rotors were performed using an instrument equipped with UV−vis detector (wave range 190−800 nm) and reversed-phase semipreparative columns LC 18. The HPLC grade solvents (CH_3CN and CH_2Cl_2) were commercially available.

*3β-[(tert-Butyldimethylsilyl)oxy]-5α-androstan-17-one (**2**).* Obtained from epiandrosterone **1** (3.62 g, 12.46 mmol) according to the literature procedure[23] in 89% yield (4.49 g) as a white crystalline material: mp 166−167 °C (lit.[23] mp 166−167 °C).

*3β-[(tert-Butyldimethylsilyl)oxy]-17α-ethynyl-5α-androstan-17β-ol (**3**).* A solution of 3β-[(*tert*-butyldimethylsilyl)oxy]-5α-androstan-17-one (**2**) (1.50 g, 3.71 mmol) in dry THF (80 mL) was placed in a flame-dried 250 mL round-bottomed flask. Then ethynylmagnesium chloride (9 mL, 0.5 M in THF, 4.5 mmol, 1.2 equiv) was added to the reaction mixture at ambient temperature. After 22 h, the reaction was quenched by slow addition of saturated NH_4Cl (100 mL). The phases were separated, and the aqueous phase was extracted twice with Et_2O (100 mL each). The combined organic layers were washed with brine, dried over Na_2SO_4, and concentrated under reduced pressure. Flash column chromatography (gradient, 98:2 to 97:3 hexane/AcOEt) afforded 1.13 g (2.62 mmol, 71% yield) of **3** as a white crystalline material: mp 186−187 °C (hexane/AcOEt): R_f = 0.46 (hexane/AcOEt 8:2); IR (cm^{-1}, $CHCl_3$) ν 3597, 3305, 2930, 2857, 1472, 1253, 1092, 836; ^1H NMR (ppm, $CDCl_3$) δ 3.60−3.50 (m, 1H), 2.57 (s, 1H), 2.32−2.24 (m, 1H), 2.18 (s, 2H), 2.01−1.93 (m, 1H), 0.89 (s, 9H), 0.84 (s, 3H), 0.82 (s, 3H), 0.71−0.63 (m, 1H), 0.05 (s, 6H); ^{13}C NMR (ppm, $CDCl_3$) δ 87.7(C), 80.0 (C), 73.8 (CH), 72.1 (CH), 54.1 (CH), 50.5 (CH), 46.9 (C), 45.1 (CH), 39.0 (CH_2), 38.7 (CH_2), 37.2 (CH_2), 36.2 (CH), 35.6 (C), 32.7 (CH_2), 31.9 (CH_2), 31.7 (CH_2), 28.6 (CH_2), 25.9 (3 × CH_3), 23.1 (CH_2), 20.9 (CH_2), 18.3 (C), 12.8 (CH_3), 12.4 (CH_3), −4.5 (2 × CH_3); HRMS (ESI) calcd for *m*/*z* $C_{27}H_{46}O_2SiNa^+$ requires 453.3165, found 453.3176.

*1,4-Bis[3β-[(tert-butyldimethylsilyl)oxy]-17β-hydroxy-5α-androstan-17α-yl-ethynyl]benzene (**4**).* A solution of tetrakis(triphenylphosphine)palladium(0) (169 mg, 0.15 mmol, 10 mol %) and 1,4-diiodobenzene (241 mg, 0.73 mmol, 0.5 equiv) in dry THF (50 mL) was placed in a flame-dried 150 mL round-bottomed flask. To the resulting homogeneous solution was added **3** (630 mg, 1.46 mmol), and the reaction mixture was heated to 40 °C. After 10 min, copper(I) iodide (28 mg, 0.15 mmol, 10 mol %) and *N*,*N*-diisopropylethylamine (1.5 mL, 8.61 mmol, 5.9 equiv) were added. After being stirred at 40 °C for 1 h, the reaction mixture was cooled to room temperature, poured into water, and extracted twice with Et_2O (100 mL each). The combined organic layers were dried over Na_2SO_4 and evaporated in vacuum. Flash column chromatography (gradient, 93:7 to 92:8 hexane/AcOEt) afforded 328 mg (0.35 mmol, 48% yield) of the linear dimer **4** as a white crystalline material: mp 243−245 °C (hexane/AcOEt); R_f = 0.42 (hexane/AcOEt 8:2); IR (cm^{-1}, $CHCl_3$) ν 3597, 2931, 2857, 1472, 1256, 1092, 837; ^1H NMR (ppm, $CDCl_3$) δ 7.38 (s, 4H), 3.59−3.50 (m, 2H), 2.40−2.32 (m, 2H), 2.09−2.01 (m, 2H), 0.89 (s, 18H), 0.89 (s, 6H), 0.83 (s, 6H), 0.72−0.64 (m, 2H), 0.06 (s, 12H); ^{13}C NMR (ppm, $CDCl_3$) δ 131.5 (4 × CH), 122.8 (2 × C), 94.7 (2 × C), 85.4 (2 × C), 80.5 (2 × C), 72.1 (2 × CH), 54.2 (2 × CH), 50.9 (2 × CH), 47.5 (2 × C), 45.1 (2 × CH), 39.1 (2 × CH_2), 38.7 (2 × CH_2), 37.2 (2 × CH_2), 36.2 (2 × CH), 35.6 (2 × C), 33.1 (2 × CH_2), 32.0 (2 × CH_2), 31.7 (2 × CH_2), 28.6 (2 × CH_2), 25.9 (6 × CH_3), 23.3 (2 × CH_2), 21.0 (2 × CH_2), 18.3 (2 × C), 13.0 (2 × CH_3), 12.4 (2 × CH_3), −4.6 (4 × CH_3); HRMS (ESI) calcd for *m*/*z* $C_{60}H_{94}O_4Si_2Na^+$ requires 957.6588, found 957.6611.

*1,4-Bis(3β,17β-dihydroxy-5α-androstan-17α-yl-ethynyl)benzene (**5**).* A solution of dimer **4** (664 mg, 0.71 mmol) in dry THF (60 mL) was placed in a 250 mL round-bottomed flask, and then tetra-*n*-butylammonium fluoride (10 mL, 1 M in THF, 4.26 mmol, 6 equiv) was added dropwise. After being stirred at room temperature for 22 h, the reaction mixture was poured into water and extracted three times with Et_2O (100 mL each) and twice with AcOEt (100 mL each). The combined organic layers were dried over Na_2SO_4, and solvents were evaporated under reduced pressure. Flash column chromatography (gradient, 6:4 to 1:1 hexane/AcOEt) afforded 487 mg (0.69 mmol, 97% yield) of linear dimer **5** as a white crystalline material: mp 285−286 °C (hexane/AcOEt); R_f = 0.49 (AcOEt); IR (cm^{-1}, KBr) ν 3356, 2936, 1508, 1448, 837. ^1H NMR (ppm, DMSO-d_6) δ 7.37 (s, 4H), 3.41−3.30 (m, 2H), 2.20−2.11 (m, 2H), 1.94−1.86 (m, 2H), 0.76 (s, 12H), 0.66−0.57 (m, 2H); ^{13}C NMR (ppm, DMSO-d_6) δ 131.4 (4 × CH), 122.5 (2 × C), 96.9 (2 × C), 83.6 (2 × C), 78.6 (2 × C), 69.3 (2 × CH), 59.7 (2 × CH_2), 53.8 (2 × CH), 50.4 (2 × CH), 47.0 (2 × C), 44.3 (2 × CH), 38.9 (2 × CH_2), 38.2 (2 × CH_2), 36.6 (2 × CH_2), 35.8 (2 × CH), 35.2 (2 × C), 32.9 (2 × CH_2), 31.4 (2 × CH_2), 28.3 (2 × CH_2), 23.0 (2 × CH_2), 20.7 (2 × CH_3), 20.6 (2 × CH_2), 14.1 (2 × CH_3); HRMS (ESI) calcd for *m*/*z* $C_{48}H_{66}O_4Na^+$ requires 729.4859, found 729.4828.

*1,4-Bis[3α-(but-3′-enoyloxy)-17β-hydroxy-5α-androstan-17α-yl-ethynyl]benzene (**6**).* Triphenylphosphine (569 mg, 2.16 mmol, 4 equiv), 3-butenoic acid (0.19 mL, 2.16 mmol, 4 equiv), and THF (50 mL) were placed together in a 250 mL round-bottomed flask. Then, dimer **5** (384 mg, 0.54 mmol) and diethyl azodicarboxylate (0.67 mL, 40% in THF, 4.25 mmol, 7.9 equiv) were added. The reaction was

dx.doi.org/10.1021/jo3020402 | J. Org. Chem. 2012, 77, 9970−9978

stirred for 18 h at room temperature. Upon concentration under reduced pressure, the crude product was poured into water and extracted twice with Et_2O (100 mL each). The combined organic layers were washed three times with a solution of ceric ammonium nitrate (100 mL each), dried over Na_2SO_4, and evaporated in vacuum. Flash column chromatography (gradient, 9:1 to 85:15 hexane/AcOEt) afforded 192 mg (0.23 mmol, 42% yield) of diester **6** as a white crystalline material: mp 215−217 °C (hexane/AcOEt); R_f = 0.49 (hexane/AcOEt 7:3); IR (cm^{-1}, $CHCl_3$) ν 3597, 2937, 2858, 1722, 1184, 1160, 988; ^1H NMR (ppm, $CDCl_3$) δ 7.40 (s, 4H), 6.00−5.90 (m, 2H), 5.20−5.16 (m, 2H), 5.15−5.13 (m, 2H), 5.05 (m, 2H), 3.09 (dt, J = 6.9, 1.4 Hz, 4H), 2.40−2.33 (m, 2H), 2.09−2.02 (m, 4H), 0.90 (s, 6H), 0.83 (s, 6H); ^{13}C NMR (ppm, $CDCl_3$) δ 171.0 (2 × C), 131.5 (4 × CH), 130.6 (2 × CH), 122.9 (2 × C), 118.2 (2 × CH_2), 94.8 (2 × C), 85.4 (2 × C), 80.4 (2 × C), 70.3 (2 × CH), 53.9 (2 × CH), 50.8 (2 × CH), 47.4 (2 × C), 40.0 (2 × CH), 39.6 (2 × CH_2), 39.1 (2 × CH_2), 36.2 (2 × CH), 35.9 (2 × C), 33.0 (2 × CH_2), 32.9 (2 × CH_2), 32.8 (2 × CH_2), 31.4 (2 × CH_2), 28.2 (2 × CH_2), 26.1 (2 × CH_2), 23.2 (2 × CH_2), 20.5 (2 × CH_2), 13.0 (2 × CH_3), 11.3 (2 × CH_3); HRMS (ESI) calcd for m/z $C_{56}H_{74}O_6Na^+$ requires m/z 865.5383, found 865.5347.

*Ring-Closing Metathesis: Synthesis of Rotors **7E** and **7Z**.* A solution of diester **6** (30 mg, 0.04 mmol) in dry toluene (200 mL) was placed under argon atmosphere in a flame-dried 500 mL round-bottomed flask, and then the reaction was heated to 80 °C. After 5 min, Grubbs second-generation catalyst (5 mg, 0.06 mmol, 15 mol %) was added. The reaction mixture was stirred for 3 h at 80 °C, cooled to room temperature, and quenched with ethylvinyl ether (1 mL). The solvents were removed under reduced pressure, and the residue was extracted three times with AcOEt (100 mL each). The combined organic layers were dried over Na_2SO_4 and evaporated in vacuo. The separation of rotors (**7a** and **7b**) from the catalyst and/or its decomposition products was performed by flash column chromatography (gradient, 85:15 to 8:2 hexane/AcOEt, on 230−400 mesh silica gel). The mixture of isomeric rotors **7a** and **7b** was obtained (19 mg, 0.023 mmol, 67% yield; E/Z ratio ~1:1, determined by ^1H NMR). The separation of the rotors was achieved by HPLC.

*Molecular Rotor **7E**.* White crystalline material: dec above 305 °C (CH_2Cl_2); R_f = 0.41 (hexane/AcOEt 7:3); HPLC t_R (9:1 CH_3CN/CH_2Cl_2) 10.91 min; IR (cm^{-1}, $CHCl_3$) ν 3595, 2933, 2858, 1721, 1265; IR (cm^{-1}, ATR) ν 3538, 2922, 2858, 1737, 1267, 1153, 987, 850; ^1H NMR (ppm, $CDCl_3$) δ 7.43 (s, 4H), 5.73 (m, 2H), 5.04 (m, 2H), 3.18−3.07 (m, 4H), 2.40−2.33 (m, 2H), 2.09−1.97 (m, 4H), 0.90 (s, 6H), 0.81 (s, 6H), 0.72−0.63 (m, 2H); ^{13}C NMR (ppm, $CDCl_3$) δ 171.1 (2 × C), 131.5 (4 × CH), 126.0 (2 × CH), 122.9 (2 × C), 94.9 (2 × C), 85.1 (2 × C), 80.2 (2 × C), 70.5 (2 × CH), 54.1 (2 × CH), 50.8 (2 × CH), 47.7 (2 × C), 40.2 (2 × CH), 39.0 (2 × CH_2), 38.8 (2 × CH_2), 36.2 (2 × CH), 35.8 (2 × C), 33.0 (2 × CH_2), 32.9 (2 × CH_2), 32.8 (2 × CH_2), 31.5 (2 × CH_2), 28.2 (2 × CH_2), 26.0 (2 × CH_2), 23.2 (2 × CH_2), 20.5 (2 × CH_2), 12.9 (2 × CH_3), 11.4 (2 × CH_3); HRMS (ESI) calcd for m/z $C_{54}H_{70}O_6Na^+$ requires 837.5070, found 837.5058.

*Molecular Rotor **7Z**.* White crystalline material: mp 299−300 °C (CH_2Cl_2/hexane); R_f = 0.41 (hexane/AcOEt 7:3); HPLC t_R (9:1 CH_3CN/CH_2Cl_2) 12.06 min; IR (cm^{-1}, $CHCl_3$) ν 3596, 2931, 2857, 1725, 1265, 1159; IR (cm^{-1}, ATR) ν 3426, 2934, 2857, 1737, 1712, 1263, 1178, 1159, 1043, 834, 742; ^1H NMR (ppm, $CDCl_3$) δ 7.41 (s, 4H), 5.87 (m, 2H), 5.07 (m, 2H), 3.16−3.06 (m, 4H), 2.40−2.32 (m, 2H), 2.09−1.95 (m, 4H), 0.90 (s, 6H), 0.82 (s, 6H), 0.74−0.65 (m, 2H); ^{13}C NMR (ppm, $CDCl_3$) δ 171.0 (2 × C), 131.4 (4 × CH), 124.0 (2 × CH), 122.9 (2 × C), 94.7 (2 × C), 85.1 (2 × C), 80.2 (2 × C), 70.4 (2 × CH), 54.2 (2 × CH), 50.9 (2 × CH), 47.6 (2 × C), 40.2 (2 × CH), 38.8 (2 × CH2), 36.1 (2 × CH), 35.9 (2 × C), 33.3 (2 × CH_2), 33.0 (2 × CH_2), 33.0 (2 × CH_2), 32.8 (2 × CH_2), 31.6 (2 × CH_2), 28.2 (2 × CH_2), 26.1 (2 × CH_2), 23.2 (2 × CH_2), 20.5 (2 × CH_2), 12.9 (2 × CH_3), 11.4 (2 × CH_3); HRMS (ESI) calcd for m/z $C_{54}H_{70}O_6Na^+$ requires 837.5070, found 837.5048.

■ ASSOCIATED CONTENT

Ⓢ Supporting Information

Spectroscopic data for compounds **3**−**7**, X-ray powder diffraction patterns, ^{13}C CPMAS and ^{13}C CPMAS non-quaternary suppression spectra of compounds **7*E*** and **7*Z***, thermogravimetric traces of **7*E*** and **7*Z***, crystallographic parameters and crystallographic information files (cif) for compounds **7*E*** and **7*Z***, alternative line shape comparisons using the ACBD array, Eyring plot of $\ln(k_{rot}/T)$ over $1000/T$ with activation enthalpy and entropy. This material is available free of charge via the Internet at http://pubs.acs.org.

■ AUTHOR INFORMATION

Corresponding Author

*E-mail: morzycki@uwb.edu.pl, mgg@chem.ucla.edu.

Notes

The authors declare no competing financial interest.

■ ACKNOWLEDGMENTS

Financial support from the Polish National Science Centre (DEC-2011/02/A/ST5/00459) and CONACyT México is gratefully acknowledged. Work at UCLA was supported by National Science Foundation Grant Nos. DMR1101934 and CHE0-844455.

■ REFERENCES

(1) (a) Mislow, K. *Chemtracts: Org. Chem.* **1988**, *2*, 151. (b) Mislow, K. *Acc. Chem. Res.* **1976**, *9*, 26. (c) Balzani, V; Credi, A.; Raymo, F. M.; Stoddart, J. F. *Angew. Chem., Int. Ed.* **2000**, *39*, 3348. (d) Karlen, S. D.; Garcia-Garibay, M. A. *Top. Curr. Chem.* **2006**, *262*, 179. (e) Liu, Y.; Flood, A. H.; Bonvallet, P. A.; Vignon, S. A.; Tseng, H.-R.; Huang, T. J.; Brough, B.; Baller, M.; Magonov, S.; Solares, S.; Goddard, W. A.; Ho, C.-M.; Stoddart, J. F. *J. Am. Chem. Soc.* **2005**, *127*, 9745. (f) Steuerman, D. W.; Tseng, H.-R.; Peters, A. J.; Flood, A. H.; Jeppesen, J. O.; Nielsen, K. A.; Stoddart, J. F.; Heath, J. R. *Angew. Chem., Int. Ed.* **2004**, *43*, 6486. (g) Shirai, Y.; Osgood, A. J.; Zhao, V.; Kelly, K. F.; Tour, J. M. *Nano Lett.* **2005**, *5*, 2330. (h) Pollard, M. M.; Klok, M.; Pijper, D.; Feringa, B. L. *Adv. Func. Mater* **2007**, *17*, 718. (i) Kelly, T. R. *Top. Curr. Chem.* **2005**, 262.

(2) (a) Kottas, G. S.; Clarke, L. I.; Horinek, D.; Michl, J. *Chem. Rev.* **2005**, *105*, 1281. (b) Michl, J.; Sykes, E. C. H. *ACS Nano* **2009**, *3*, 1042.

(3) (a) Salech, B. E. A.; Teich, M. C. *Fundamentals of Photonics*; Wiley-Interscience: New York, 1991. (b) Blinov, L. M. *Electro-Optic and Magneto-Optical Properties of Liquid Crystals*; Wiley: New York, 1983. (c) Newnham, R. E. *Properties of Materials, Anisotropy, Symmetry and Structure*; Oxford University Press: New York, 2005.

(4) (a) Dominguez, Z.; Dang, H.; Strouse, M. J.; Garcia-Garibay, M. A. *J. Am. Chem. Soc.* **2002**, *124*, 2398. (b) Dominguez, Z.; Dang, H.; Strouse, J. M.; Garcia-Garibay, M. A. *J. Am. Chem. Soc.* **2002**, *124*, 7719. (c) Horansky, R. D.; Clarke, L. I.; Price, J. C.; Khuong, T.-A. V.; Jarowski, P. D.; Garcia-Garibay, M. A. *Phys. Rev. B.* **2005**, *B72*, 014302. (d) Horansky, R. D.; Clarke, L. I.; Winston, E. B.; Price, J. C.; Karlen, S. D.; Jarowski, P. D.; Santillan, R.; Garcia-Garibay, M. A. *Phys. Rev. B* **2006**, *74*, 054306.

(5) For additional examples of molecular gyroscopes in the literature please see: (a) Skopek, K.; Hershberger, M. C.; Gladysz, J. A. *Coord. Chem. Rev.* **2007**, *251*, 1723. (b) Setaka, W.; Yamaguchi, K. *J. Am. Chem. Soc.* **2012**, *134*, 12458. (c) Khan, N. S.; Perez-Aguilar, J. M.; Kaufmann, T.; Hill, P. A.; Taratula, O.; Lee, O. S.; Carroll, P. J.; Saven, J. G.; Dmochowski, I. J. *J. Org. Chem.* **2011**, *76*, 1418.

(6) Dominguez, Z.; Khuong, T.-A. V.; Sanrame, C. N.; Dang, H.; Nuñez, J. E.; Garcia-Garibay, M. A. *J. Am. Chem. Soc.* **2003**, *125*, 8827.

(7) (a) Garcia-Garibay, M. A. *Proc. Natl. Acad. Sci. U.S.A.* **2005**, *102*, 10793. (b) Khuong, T.-A. V.; Nuñez, J. E.; Godinez, C. E.; Garcia-Garibay, M. A. *Acc. Chem. Res.* **2006**, *39*, 413.

(8) Lemouchi, C.; Vogelsberg, C. S.; Zorina, L.; Simonov, S.; Batail, P.; Brown, S.; Garcia-Garibay, M. A. *J. Am. Chem. Soc.* **2011**, *133*, 6371.
(9) (a) Vogelsberg, C. S.; Garcia-Garibay, M. A. *Chem. Soc. Rev.* **2012**, *41*, 1892. (b) Arcos-Ramos, R.; Rodríguez-Molina, B.; Romero, M.; Méndez-Stivalet, J. M.; Ochoa, M. E.; Ramírez-Montes, P. I.; Santillan, R.; Garcia-Garibay, M. A.; Farfán, N. *J. Org. Chem.* **2012**, *77*, 6887.
(10) Rodríguez-Molina, B.; Pozos, A.; Cruz, R.; Romero, M.; Flores, B.; Farfán, N.; Santillan, R.; Garcia-Garibay, M. A. *Org. Biomol. Chem.* **2010**, *8*, 2993.
(11) Rodríguez-Molina, B.; Romero, M.; Méndez-Stivalet, J. M.; Farfán, N.; Santillan, R.; Garcia-Garibay, M. A. *J. Am. Chem. Soc.* **2011**, *133*, 7280.
(12) Centore, R.; Jazbinsek, M.; Tuzi, A.; Roviello, A.; Capobianco, A.; Peluso, A. *CrystEngComm* **2012**, *14*, 2645.
(13) (a) Rosenkranz, G.; Pataki, J.; Djerassi, C. *J. Am. Chem. Soc.* **1951**, *73*, 4055. (b) Marker, R. E.; Wagner, R. B.; Ulshafer, P. R.; Wittbecker, E. L.; Goldsmith, D. P. J.; Ruof, C. H. *J. Am. Chem. Soc.* **1947**, *69*, 2167.
(14) (a) Chapelon, A.-S.; Moraléda, D.; Rodriguez, R.; Ollivier, C.; Santelli, M. *Tetrahedron* **2007**, *63*, 11511. (b) D'herde, J. N.; De Clercq, P. J. *Molecules* **2006**, *11*, 655. (c) Jiang, B.; Shi, H.-P.; Xu, M.; Wang, W.-J.; Zhou, W.-S. *Tetrahedron* **2008**, *64*, 9738.
(15) (a) Davis, A. P. *Chem. Soc. Rev.* **1993**, 243. (b) Li, Y.; Dias, J. R. *Chem. Rev.* **1997**, *97*, 283. (c) Wallimann, P.; Marti, T.; Furer, A.; Diederich, F. *Chem. Rev.* **1997**, *97*, 1567. (d) Tamminen, J.; Kolehmainen, E. *Molecules* **2001**, *6*, 21. (e) Davis, A. P.; Joos, J. B. *Coord. Chem. Rev.* **2003**, *240*, 143.
(16) Simoes, C. M. O.; Amoros, M.; Girre, L. *Phytother. Res.* **1999**, *13*, 323.
(17) Killeen, G. F.; Madigan, C. A.; Connolly, C. R.; Walsh, G. A.; Clark, C.; Hynes, M. J.; et al. *J. Agric. Food. Chem.* **1998**, *46*, 3178.
(18) Sindambiwe, J. B.; Calomme, M.; Geerts, S.; Pieters, L.; Vlietinck, A. J.; Vanden Berghe, D. A. *J. Nat. Prod.* **1998**, *61*, 585.
(19) (a) Itabashi, M.; Segawa, K.; Ikeda, Y.; Kondo, S.; Naganawa, H.; Koyano, T.; et al. *Carbohydr. Res.* **1999**, *323*, 57. (b) Yu, W.; Jin, Z. *J. Am. Chem. Soc.* **2001**, *123*, 3369. (c) Deng, S.; Yu, B.; Lou, Y.; Hui, Y. *J. Org. Chem.* **1999**, *64*, 202. (d) Yu, W.; Jin, Z. *J. Am. Chem. Soc.* **2002**, *124*, 6576.
(20) (a) Chhatra, R. K.; Kumar, A.; Pandey, P. S. *J. Org. Chem.* **2011**, *76*, 9086. (b) Bai, X.; Barnes, C.; Pascal, C. B.; Chen, X.; Dias, J. R. *Org. Lett.* **2011**, *13*, 3064. (c) Gautrot, J. E.; Zhu, X. X. *J. Mater. Chem.* **2009**, *19*, 5705.
(21) (a) Bernstein, J. *Polymorphism in Organic Chemistry*; Oxford University Press: Oxford, 2002. (b) Bernstein, J. In *Solid State Organic Chemistry*; Desiraju, G., Ed.; Elsevier: Amsterdam, 1987; pp 471−518.
(22) Morzycki, J. W. *Steroids* **2011**, *76*, 949.
(23) (a) Felzmann, W.; Gmeiner, G.; Gartner, P. *Steroids* **2005**, *70*, 103. (b) Bruttomesso, A. C.; Doller, D.; Gros, E. G. *Synth. Commun.* **1998**, *28*, 4043.
(24) (a) Fieser, L. F.; Fieser, M. *Steroids*; Reinhold Publishing Corp.: New York, 1959; p 467. (b) Kanojia, R. M.; Allen, G. O.; Killinger, J. M.; McGuire, J. L. *J. Med. Chem.* **1979**, *22*, 1538. (c) Wong, F. F.; Chuang, S. H.; Yang, S.; Lin, Y.-H.; Tseng, W.-C.; Lin, S.-K.; Huang, J.-J. *Tetrahedron* **2010**, *66*, 4068.
(25) (a) Mitsunobu, O. *Synthesis* **1981**, 1. (b) Hughes, D. L. The Mitsunobu Reaction. In *Organic Reactions*; Beak, P., et al., Eds.; John Wiley & Sons, Inc.: New York, 1992; Vol. *42*, p 335.
(26) (a) Vatèle, J.-M. *Tetrahedron* **2007**, *63*, 10921. (b) Gong, H.; Williams, J. R. *Org. Lett.* **2006**, *8*, 2253. (c) Di Filippo, M.; Izzo, I.; Raimondi, S.; De Riccardis, F.; Sodano, G. *Tetrahedron Lett.* **2001**, *42*, 1575.
(27) HyperChemTM, Release 3 from Hypercube, Inc.; minimizations employed the MM+ force field and the Polak−Ribiere (conjugate gradient) algorithm.
(28) Harada, J.; Ogawa, K. *Chem. Soc. Rev.* **2009**, *38*, 2244.
(29) Steiner., T. *Angew. Chem., Int. Ed.* **2002**, *41*, 48.
(30) Sandstrom, J. *Dynamic NMR Spectroscopy*; Academic Press: London, 1982.
(31) (a) Alemany, L. B.; Grant, D. M.; Alger, T. D.; Pugmire, R. J. *J. Am. Chem. Soc.* **1983**, *105*, 6697. (b) Opella, S. J.; Frey, M. *J. Am. Chem. Soc.* **1979**, *101*, 5854. (c) Opella, S. J.; Frey, M. H.; Cross, T. A. *J. Am. Chem. Soc.* **1979**, *101*, 5856.
(32) WinDNMR software, v. 7.1.13. Reich, H. J. *J. Chem. Educ.* **1995**, *72*, 1086.
(33) Hoping simulations between sites related by 180° were carried out using a 2 × 2 spin model, with chemical shifts varying ± 0.06% as compared with the experimental data and a FWHM between 45 and 60 Hz with an asymmetry of 52.5/47.5 constant over the whole temperature interval. See the Supporting Information for the resulting features using the alternative arrangement ACBD.